Importance and origin of halosteric contribution to sea level change in the southeast Indian Ocean during 2005-2013

W. Llovel, Tong Lee

AGU PUBLICATIONS

Geophysical Research Letters

RESEARCH LETTER

10.1002/2014GL062611

Key Points:
- Importance of halosteric contribution to sea level change
- Halosteric contribution associated with an upper ocean freshening
- Importance of the Maritime Continent and the Indonesian throughflow

Correspondence to:
W. Llovel,
william.llovel@cerfacs.fr

Citation:
Llovel, W., and T. Lee (2015), Importance and origin of halosteric contribution to sea level change in the southeast Indian Ocean during 2005–2013, *Geophys. Res. Lett.*, *42*, 1148–1157, doi:10.1002/2014GL062611.

Received 25 NOV 2014
Accepted 22 JAN 2015
Accepted article online 23 FEB 2015
Published online 26 FEB 2015

Importance and origin of halosteric contribution to sea level change in the southeast Indian Ocean during 2005–2013

William Llovel[1,2] and Tong Lee[1]

[1]Jet Propulsion Lab, Caltech, Pasadena, California, USA, [2]University California Los Angeles, Joint Institute for Regional Earth System Science & Engineering, Los Angeles, California, USA

Abstract Steric sea level change has been identified as one of the major contributors to the regional variability of sea level trends observed by satellite altimetry for the past two decades. This contribution varies in space and time. The temperature (thermosteric) contribution to sea level has generally been found to be more important than the salinity (halosteric) effect. Based on sea level measurements from satellite altimetry and temperature and salinity data from Argo floats during 2005–2013, we found that the southeast Indian Ocean experiences a large halosteric contribution to sea level change. The conspicuously large halosteric contribution is associated with a freshening in the upper 300 m. Neither local atmospheric forcing such as Ekman pumping and $E - P$ nor halosteric signal transmitted from the western tropical Pacific can explain this freshening. An enhanced precipitation in the Maritime Continent region and the observed strengthening of the Indonesian throughflow are the likely causes.

1. Introduction

Sea level change is an important consequence of climate change that has significant societal and economical implications [*Nicholls and Cazenave*, 2010]. Global mean sea level rise is a result of ocean warming and fresh water mass inputs from the melting of land ice [*Church et al.*, 2013]. This rise is expected to continue for decades to come as the Earth's climate is projected to continue to warm [*Collins et al.*, 2013; *Kirtman et al.*, 2013]. A better understanding of the physical processes involved in the regional patterns of sea level for the past years and decades is necessary to assess the reliability of climate models and related future projections. Sea level change varies in space and time. Regional sea level trends display a nonuniform pattern in the past two decades, as revealed by satellite altimetry data [*Cazenave and Llovel*, 2010]. These spatial patterns can be explained in part by temperature changes in the upper ocean [*Stammer et al.*, 2013]. In contrast to global sea level rise where temperature change is a main factor, regional sea level changes are also affected by salinity variations, which could enhance or compensate the effect of temperature [*Griffies and Greatbatch*, 2012]. Addition of fresh water mass from continent ice melting can also contribute to the regional variability of sea level trends [*Lorbacher et al.*, 2012]. The addition of mass contributes to about 68% of the net global mean sea level rise for the last decade from 2005 to 2013 [*Llovel et al.*, 2014]. Ocean circulation and geophysical processes (postglacial rebound) also influence the pattern of sea level changes [*Stammer et al.*, 2013].

The salinity contribution to regional sea level trends has been less studied than the temperature contribution because the halosteric contribution to mean sea level is close to zero [*Gregory and Lowe*, 2000], also due to the lack of historical salinity measurements and because salinity anomalies are more important for sea level change on shorter time scales [*Wunsch et al.*, 2007; *Köhl*, 2014]. The development of the International Argo program has provided indispensible salinity measurements to quantify regional halosteric contributions [*Gould et al.*, 2004]. Since 2005, the majority of the world ocean (ice-free outside marginal seas) is monitored [*Roemmich and Gilson*, 2009]. Argo data record has now reached almost a decade offering the opportunity to investigate decadal change of temperature and salinity contributions to sea level variations.

This study uses Argo temperature and salinity observations and sea level measurements obtained from satellite altimetry to characterize the spatial patterns of thermosteric and halosteric effects on regional sea level trends during 2005–2013. In particular, we identify the southeast Indian Ocean as a region where halosteric contribution dominates steric sea level change during the Argo era. We also examine the origin of large halosteric sea level change in this region by investigating the potential roles of local and remote forcing.

The Indian Ocean is surrounded by highly populated areas containing about one third of the world's population, mostly living in developing countries [*Han et al*., 2014]. Therefore, understanding decadal variability and future regional sea level rise is an important task to predict the future socioeconomical impacts for the rim countries. However, decadal climate variability in the Indian Ocean sector has not been studied as extensively [*Han et al*., 2014] as those in the Atlantic and Pacific sectors [*Liu*, 2012]. Therefore, our study also provides a significant contribution to the knowledge of decadal variability of the Indian Ocean.

This paper is organized as follows. The data sets used in the analysis are described in section 2. In section 3, we present our results on the upper ocean freshening to sea level changes for the southeast Indian Ocean with a following section discussing the possible local and remote forcing of such a change. Finally, we summarize the results, address the broader implications of the findings, and discuss the future work motivated by this study.

2. Data and Methods

2.1. Sea Level Data

The sea level data analyzed in this study are the Ssalto/duacs multimission sea level products provided by CLS/Archiving, Validation, and Interpretation of Satellite Oceanographic data (AVISO). The 1/4° × 1/4° resolution, daily maps were used. We have used the data set based on only two missions, at most, with relatively homogeneous ground tracks for the entire period of the study. The data used in this study span from January 2005 to December 2013. Geophysical and environmental corrections have been applied to the data [*Ablain et al*., 2009].

2.2. Temperature and Salinity Gridded Products

The temperature and salinity products we used are the Argo-based temperature- (T) and salinity- (S) gridded fields produced by the Scripps Institution of Oceanography (updated from *Roemmich and Gilson* [2009]). The T and S profiles from Argo floats have been passed through several quality control processes [*Argo data management*, 2011] and are available to standard levels. We computed thermosteric, halosteric, and steric sea level time series from the surface down to 1975 dbar depth between 64.5°N and 64.5°S at monthly interval on a 1° × 1° grid for the period of January 2005 to December 2013 by integrating the density anomalies (defined as differences between the density estimate and a reference density at 0°C and 35 Practical Salinity Scale 1978 (PSS-78) salinity using the equation of state of seawater EOS-80; *Llovel et al*. [2013]) at each standard depth.

2.3. Surface Forcing Products

Wind-induced Ekman pumping causes heaving movements of the subsurface pycnoclines, inducing variations of temperature and salinity leading to changes in thermosteric and halosteric sea level. Surface heat flux and freshwater flux (evaporation minus precipitation, hereafter noted $E-P$) affect upper ocean T and S to influence thermosteric and halosteric sea level variations. To diagnose the roles of atmospheric forcing on the conspicuously large halosteric changes we found in the southeast Indian Ocean, we focused on the analysis of Ekman pumping and $E-P$.

The 10 m wind, precipitation and evaporation data are obtained from ERA-Interim atmospheric reanalysis produced by the European Centre for Medium-Range Weather Forecasts [*Dee et al*., 2011]. The ERA-Interim data are sampled every 6 h on a global grid with approximate resolution of 1.5°. We used the data from January 2005 to December 2013. We compute the monthly estimate by averaging the 6-hourly data available for each month. Wind stress is computed following the equations:

$$\tau_x = \rho_a C_D W U_{10}$$

$$\tau_y = \rho_a C_D W V_{10}$$

where (τ_x, τ_y) represents the zonal and meridional wind stress, ρ_a the mean air density equal to 1.3 g/m^3, C_D is the Drag coefficient, determined following the wind speed-dependent formula proposed by

Large and Pond [1981], and $W = \sqrt{U_{10}^2 + V_{10}^2}$ (the wind speed at 10 m). Ekman pumping velocity is defined as

$$\overrightarrow{w_e} = -\frac{\nabla \times \overrightarrow{\tau}}{\rho_0 f}$$

where w_e represents the Ekman pumping and ρ_0 is the mean density of seawater. Note that the seawater density has been computed using Argo-based *T*- and *S*-gridded fields for each month over 2005–2013.

To examine the robustness of wind forcing estimate, we have also analyzed the 10 m wind data from National Centers for Environmental Prediction (NCEP)-Department of Energy Reanalysis II (hereafter NCEP2) [*Kanamitsu et al*., 2002]. The data are provided over a global grid with approximate spatial resolution of 2°. For evaporation, we have also analyzed the objectively analyzed air-sea fluxes (OAFlux) data produced by Woods Hole Oceanographic Institution (WHOI) [*Yu et al*., 2008]. We have downloaded the monthly estimate provided at a global 1° × 1° grid. For the precipitation, we have analyzed the Global Precipitation Climatology Project (GPCP) [*Adler et al*., 2003] that combines observations and satellite precipitation data at a 2.5° × 2.5° global grid. All data products analyzed are for the period of January 2005 to December 2013.

3. Results

3.1. Sea Level Trends

Figure 1a shows the regional patterns of observed sea level trends estimated from satellite altimetry data from 2005 to 2013. Because we are focusing on the trend over the period of the study, we have removed the monthly climatology of the time series at each location to facilitate the estimation of the uncertainty associated with the trend without the climatological seasonal cycle. The monthly climatology was computed by averaging the same calendar month of different years during 2005–2013. To highlight the regions where the trends are significant, we have marked the region where the trends are not significant at 2 standard errors with black dots. The standard errors were estimated from linear regression to the time series. We apply the same method for estimating trend errors throughout the presentation in the manuscript, unless otherwise stated.

Figure 1a highlights the regional pattern of sea level change with some regions exhibiting trends that are 3–4 times larger than the global average (Indo-Pacific region, South Pacific Ocean) while some other regions experiencing sea level drop (the Gulf of Alaska, southeastern Pacific Ocean). Figure 1b shows the map of steric sea level trends for the same time period, which represents the temperature and salinity contributions to sea level variations estimated for the upper 1975 dbar from the Argo-gridded product. The patterns of steric sea level trends (Figure 1b) are in good agreement with those of sea level trends (Figure 1a). This is consistent with previous findings [*Willis et al*., 2008; *Llovel et al*., 2010; *Cazenave and Llovel*, 2010; *Stammer et al*., 2013]. Some differences between the observed trends of sea level and estimated trends of steric sea level are found that could be attributed to ocean mass changes and/or deep ocean contribution below 1975 dbar [*Llovel et al*., 2014].

Figures 1c and 1d show the maps of thermosteric and halosteric sea level trends, respectively. The patterns of the thermosteric sea level trends (Figure 1c) are similar to those of steric sea level trends (Figure 1b). This confirms the previous findings [*Cazenave and Llovel*, 2010; *Stammer et al*., 2013] about the overall dominant contribution of temperature changes on regional sea level changes. Over much of the world ocean, halosteric sea level trends (Figure 1d) are smaller and compensate the thermosteric trends. However, halosteric trends in the southeast Indian Ocean are larger than the thermosteric trends and reenforce the latter. A more quantitative description is provided in the next paragraph. This substantial contribution of halosteric effect in this region is in stark contrast to the rest of the global ocean.

To further investigate the importance of salinity variations to regional sea level trends in the southeast Indian Ocean, we defined a mask region where halosteric sea level trend values are higher than 4 mm/yr, which is approximately the threshold where the halosteric sea level trends are significant at 2 standard errors. This region is indicated by the grey contour line in Figure 1d. Figure 2a (left) shows the time series based on spatial averages within the aforementioned mask for the observed sea level and estimated steric sea level (black and grey curves, respectively). In this region, the estimated linear trend of satellite-based sea level rise is 9.95 ± 0.95 mm/yr. This is explained almost entirely by the steric sea level contribution, 10.14 ± 1.22 mm/yr (the uncertainty represents 2 standard errors). This regional mean steric sea level trend is due to both temperature and salinity changes (Figures 2a, middle, and 2a, right) that account for 3.72 ± 1.04 mm/yr and 6.41 ± 0.62 mm/yr. Therefore, the halosteric contribution in this region is almost twice as large as the thermosteric sea level contribution. The halosteric contribution shows a quasi-linear increase starting in early 2007.

To investigate the temperature and salinity contributions to sea level change as a function of depth, we computed the yearly mean temperature, salinity, and density profiles spatially averaged within the marked region shown in Figure 1d. These yearly mean profiles are shown in Figure 2b for temperature, salinity, and density (left–right, respectively). The profiles for 2005–2007 are indicated by the black curves while those for 2008–2010 and 2011–2013 are denoted by the green and red curves, respectively. For each color group of three curves, the thick, dashed, and thin curves represent the first–third years, respectively. We show only the data in the upper 800 m because the changes below that depth are very small. Figure 2b (left) suggests that temperature in the upper 400 m experienced a warming, leading to a deepening of the thermocline from 2005 to 2013. On the other hand, Figure 2b (middle) shows a substantial freshening down to 300 m during this period, which is responsible for the increase of halosteric sea level trends that reenforces the sea level trend in that region. Figure 2b (right) shows a

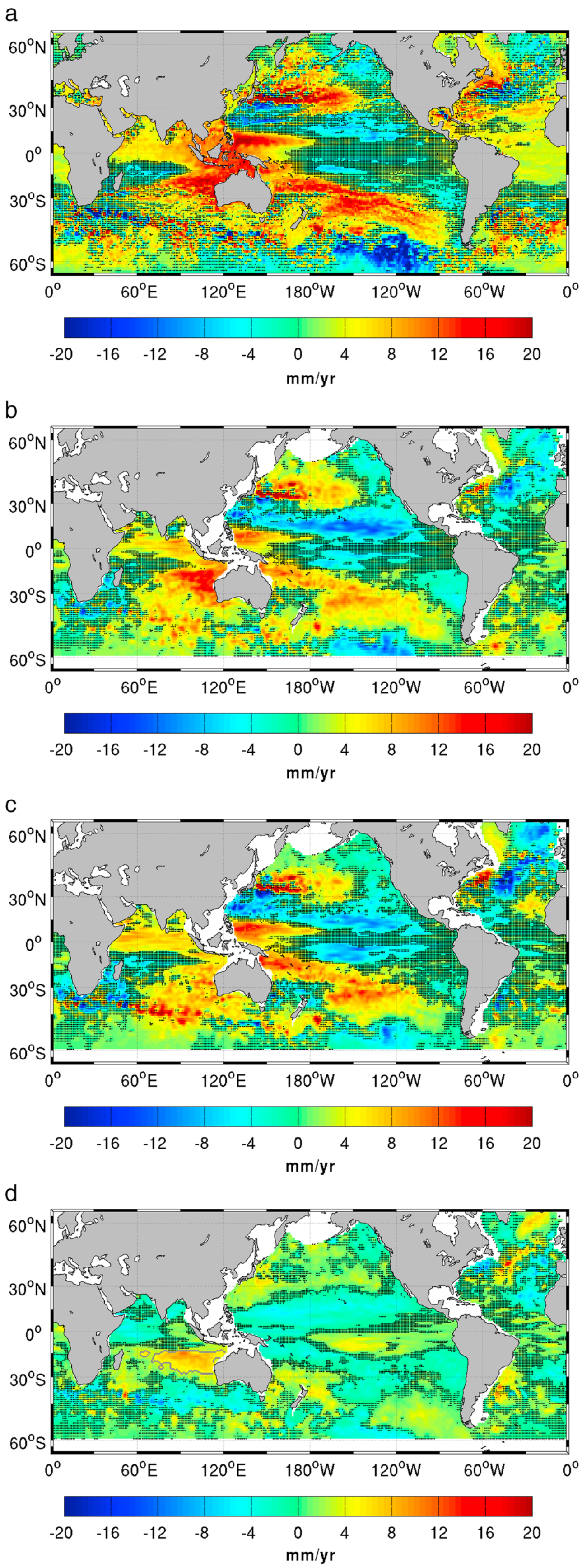

Figure 1. Sea level trend maps over 2005–2013 for (a) observed by satellite altimetry, (b) Argo-based steric sea level, (c) Argo-based thermosteric sea level, and (d) Argo-based halosteric sea level (The mask defines the region where halosteric sea level trends are higher than 4 mm/yr.). Time series have been corrected for annual signal and are referenced to the time mean computed over 2005–2013. Stippled regions denote trend estimates nonsignificant from zero at 2 standard error uncertainty.

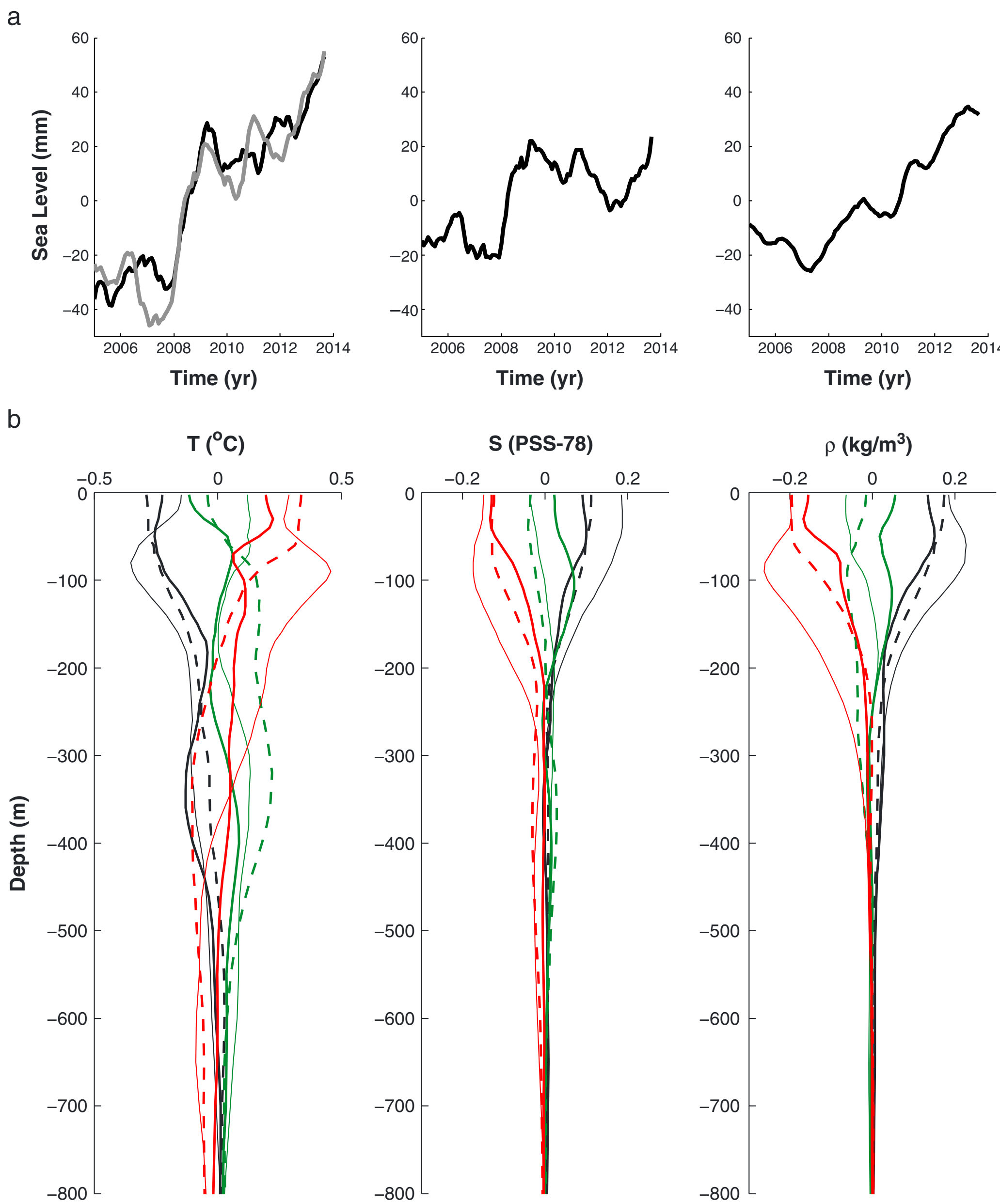

Figure 2. (a) Regional mean (left) sea level and steric component (black and grey curves, respectively), (middle) thermosteric contribution, and (right) halosteric contribution. A 7 month running mean has been applied to those curves. (b) Time evolution of yearly (left) mean temperature, (middle) mean salinity, and (right) density. The black, green, and red colors represent the yearly mean estimates for 2005–2007, 2008–2010, and 2011–2013, respectively. For each triplet, the thick, dashed, and thin lines represent the first–third years, respectively. All curves are computed over the mask in the South Indian Ocean overlaid in Figure 1d from 2005 to 2013. Annual signals have been removed and the curves are referenced to the time mean computed over 2005–2013.

decrease in density for the upper 300 m depth consistent with the temperature and salinity anomaly profiles described previously.

3.2. Local Versus Remote Forcing

A question that comes up naturally from the results presented above is the origin of the upper ocean freshening in the southeast Indian Ocean. In this section, we investigate the potential influences of local and remote forcings on this freshening. Salinity variations can be due to changes in regional river runoff, local

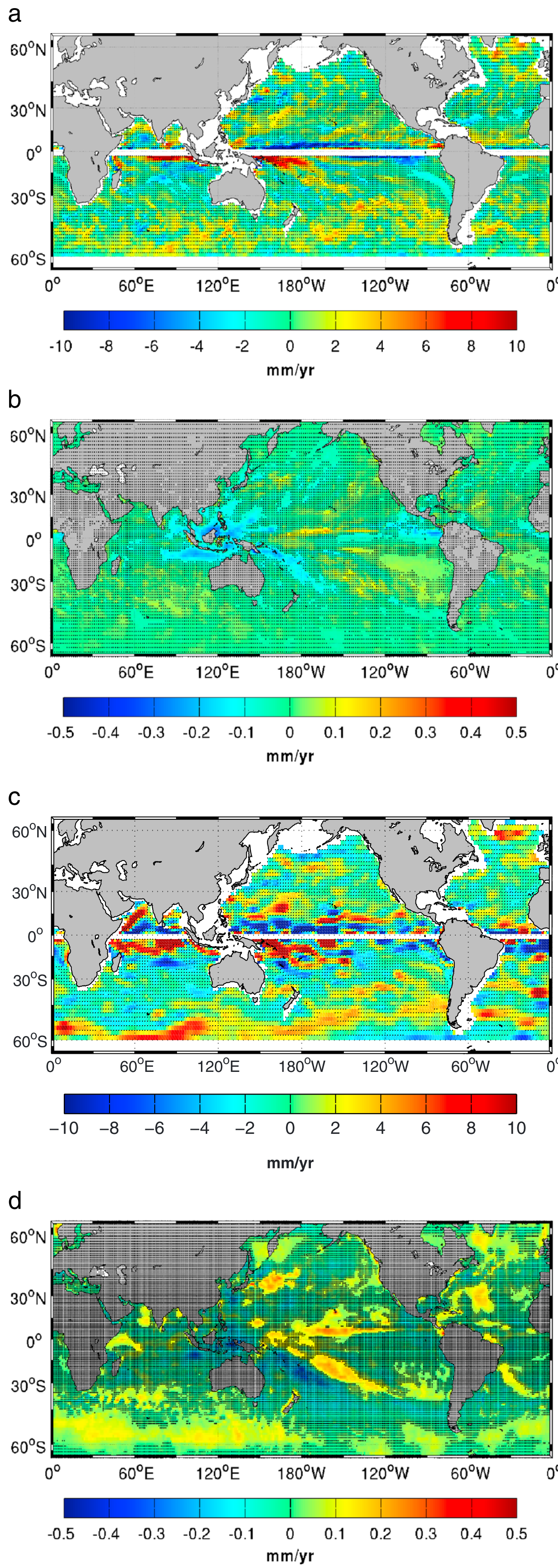

atmospheric forcing such as Ekman pumping and $E-P$, and contribution from ocean dynamics due to remote forcing. As there is no major river discharge in the rim of the southeast Indian Ocean, we can neglect the possible contribution of fresh water coming from regional river runoff. Local atmospheric forcing can be either due to changes in Ekman pumping or surface freshwater flux (i.e., $E-P$). To examine these factors, we examine the trends of Ekman pumping (from ERA-Interim and NCEP2 reanalyzes, Figures 3a and 3c) and $E-P$ (from ERA-interim reanalysis and OAFlux combined with GPCP Figures 3b and 3d). Ekman pumping is not well defined near the equator as the Coriolis parameter approaches zero. We therefore excluded the Ekman pumping estimates within 2° of the equator. The sign convention for the trend estimates is such that a positive (negative) value of trend corresponds to upward (downward) vertical velocity for Ekman pumping and ocean losing (gaining) fresh water for $E-P$. Trend values not significant at 2 standard error levels were marked by black dots in Figure 3.

In the southeast Indian Ocean, the Ekman pumping trends show different spatial patterns from the two reanalyses (Figures 3a and 3c) that are mostly not statistically different from zero. Interestingly, Figure 3c shows a region of significant negative Ekman pumping trends (based on NCEP2 reanalysis) centered to the southeast Indian Ocean. Unfortunately, this pattern is not confirmed with ERA-Interim reanalysis. Therefore, the trends of Ekman pumping cannot explain the upper ocean freshening in the southeast Indian Ocean. Were Ekman pumping the cause of the steric sea level trends in the southeast

Figure 3. Ekman pumping trend maps from (a) ERA-Interim and (c) NCEP2 reanalysis and $E-P$ from (b) ERA-Interim and (d) OAFlux combined with GPCP computed over 2005–2013. Time series have been corrected from annual signal and are referenced to the time mean computed over 2005–2013. Stippled regions denote trend estimates nonsignificant from zero at 2 standard error uncertainty.

Indian Ocean, one would expect enhanced changes near the center of the thermocline/halocline/pycnocline (approximately 150 m for the region) that reflect the first baroclinic mode response. However, Figure 2b suggests that this is not the case because the changes are largest in the upper 100 m. This is consistent with the insignificant trends of Ekman pumping inferred from the reanalysis wind products.

The $E-P$ trends have a narrow band of significant values (for ERA-Interim, Figure 3b) in southeast Indian Ocean between approximately 5°S and 10°S that corresponds to a freshening effect. Figure 3d (combined OAFlux and GPCP estimate of $E-P$ trends) also shows negative trend values located in the same region but are not significant. This band is mostly north of latitude ranges of the area with freshening that extends from approximately 14°S and 30°S as indicated in Figure 1d. Therefore, local $E-P$ cannot explain the extensive area of freshening in the southeast Indian Ocean.

Steric height changes in the southeast Indian Ocean can also be affected by those in the northwest tropical Pacific through either advection or wave propagation. Based on direct velocity measurements in the Indonesian Seas [*Gordon et al.*, 2010], the typical advective time scale from the entrance of the Indonesian throughflow (ITF) near the northwest Pacific Ocean to the exit to the Indian Ocean is less than a year (A. L. Gordon, personal communication, 2014). In other words, it would take less than a year for steric signals from the northwest Pacific near the ITF entrance to be advected to the exit to the Indian Ocean. The advection by the South Equatorial Current in the South Indian Ocean can further carry the signals toward the west at tropical latitudes. Interannual and decadal signals of sea level or thermocline signals from the northwest Pacific can also transmit through the Indonesian Seas and along the northwest coast of Australia via coastal Kelvin waves with a typical time scales of several months [*Wijffels and Meyers*, 2004; *Cai et al.*, 2005; *Lee and McPhaden*, 2008; *Feng et al.*, 2010]. Once reaching the coastal region off the northwest coast of Australia near the Leeuwin Current region, these signals can propagate toward the west either as Rossby waves at tropical latitudes or as nonlinear eddies at subtropical latitudes [*Chelton and Schlax*, 1996; *Birol and Morrow*, 2003; *Morrow et al.*, 2004]. If the steric changes in the southeast Indian Ocean are influenced remotely by the northwest Pacific, one would expect to see changes of a similar sign in the latter region. Figure 1c indeed shows evidence of remote effect of the northwest tropical Pacific on the southeast Indian Ocean for the thermosteric changes. Similar changes on longer time scales have been discussed by previous studies [*Schwarzkopf and Böning*, 2011]. However, there is no evidence of such a remote influence of halosteric change that links the northwest Pacific and southeast Indian Ocean (Figure 1d).

The fact that neither local forcing nor remote influence from the Pacific sector can explain the large halosteric changes in the southeast Indian Ocean implicates the forcing from the Maritime Continent region. This region is associated with large freshwater input due to river runoff and monsoon rainfall. For intense, the northwest Australian region and the South China Sea are large reservoirs of freshwater because of the discharges by many river systems. The South China Sea plays an important role in regulating the ITF and the water mass properties of the Indonesian Seas [*Gordon et al.*, 2003; *Qu et al.*, 2005; *Tozuka et al.*, 2007; *Gordon et al.*, 2012]. Strong tidal mixing within the Indonesian Seas plays a crucial role to modify the characteristics of water masses en route from the Pacific to the Indian Ocean [*Koch-Larrouy et al.*, 2010; *Sprintall et al.*, 2014]. *Koch-Larrouy et al.* [2010] showed that the inclusion of a tidal mixing parameterization in a climate model resulted in a cooler and freshwater outflow into the southeast Indian Ocean at the thermocline level of 100–200 m. Therefore, if there is an enhanced freshwater input from the Maritime Continent region such as the South China Sea, the strong tidal mixing in the Indonesian Seas could spread the freshening effect into greater depths. The resultant signals from the Indonesian Seas could then influence the halosteric sea level changes in the southeast Indian Ocean via an advective process, wave and eddy propagations, or a combination of these processes. Figure 3b shows significant negative trends of $E-P$ in the Maritime Content region. These negative trends are primarily due to the trend of P rather than that of E (not shown). This pattern is confirmed by Figure 3d; however, the values are not statistically different from zero. The possible enhancement of precipitation in the Maritime Continent region as inferred from the ERA-Interim reanalysis and combined OAFlux and GPCP estimate requires further investigation. If it is a robust feature, the cause for the enhanced precipitation during this period also needs to be investigated.

The surface freshwater water flux within the Maritime Continent region and the potential changes of river discharges in this region may not be the only factors influencing the freshening of the southeast Indian Ocean. Changes of the regional ocean currents in the region such as the ITF may also contribute. *Gordon et al.* [2012]

found that the vertical profile of the Makassar Strait throughflow, the main branch of the ITF, changed abruptly since 2007. The abrupt changes were associated with an increase of maximum thermocline velocity from 0.7 to 0.9 m/s and a shoaling of the velocity maximum from 140 m to 70 m. These correspond to a 47% increase of volume transport between 50 and 150 m during boreal spring when the ITF is the seasonally the strongest. The onset of the freshening trend of the upper southeast Indian Ocean around 2007 (Figure 2a) may be related to this change in the ITF as more (fresher) waters from the Indonesian Seas were advected out of the Indonesian Seas by the strengthened ITF.

4. Conclusions and Discussion

In this study, we have investigated the temperature and salinity contributions to regional sea level trends over the global ocean during 2005–2013. The patterns of steric sea level trends are very similar to the observed sea level trends (consistent with the results reported by *Llovel et al*. [2010] over a shorter time period) and are mostly explained by temperature changes. Over much of the world ocean, salinity generally has a secondary effect on regional sea level change. In stark contrast to the rest of the world ocean, however, the southeast Indian Ocean stands out as a region where the halosteric effect has a dominant contribution to regional sea level change. The halosteric contribution is almost twice as large as the thermosteric contribution in that region. This large halosteric contribution is associated with a freshening in the upper 300 m of the ocean.

Local forcing in the southeast Indian Ocean and remote influence from the northwest Pacific Ocean cannot explain the freshening of the southeast Indian Ocean. The possible enhanced precipitation within the Maritime Continent region and the observed strengthening of the Makassar Strait throughflow (a main branch of the ITF) since 2007 may have caused the freshening of the southeast Indian Ocean. Our finding implies an enhanced freshwater transport from the exit of the ITF into the Indian Ocean during the period of the study. The observed enhancement of ITF transport since 2007 may be an important factor as the fresher waters in the Indonesian Seas are pushed out at a faster rate. The deficit of $E - P$ (due to enhanced precipitation) inferred from ERA-Interim reanalysis and combined OAFlux and GPCP estimate may also contribute. However, the robustness of the $E - P$ estimates requires further investigation due to the relatively large uncertainty associated with reanalysis [*Dee et al*., 2011]. Further investigations are needed to understand the exact processes, such as advection, mixing, and propagation of waves and eddies, both within the Indonesian Seas and in the southeast Indian Ocean.

Decadal and multidecadal variabilities of sea level in the Indian Ocean, the associated thermocline variability, and the relative influences of local and remote forcing have been investigated by a suite of studies [*Lee*, 2004; *Lee and McPhaden*, 2008; *Han et al*., 2010; *Feng et al*., 2010; *Schwarzkopf and Böning*, 2011; *Trenary and Han*, 2013; *Nidheesh et al*., 2013]. In particular, influences of the ITF and the effects of remote forcing from the tropical Pacific sector on the southeast Indian Ocean have been discussed. *Han et al*. [2014] provided a review of the previous research on decadal and multidecadal variability of the Indian Ocean. None of the previous studies of decadal sea level changes in the Indian Ocean focused on the Argo era, a period with abundant subsurface salinity observations. Our results suggest that salinity plays an important role in decadal sea level changes in the southeast Indian Ocean. Whether this happens to be the case during the Argo period or is a more ubiquitous feature in the past few decades that have not been resolved due to the lack of in situ observations remains to be investigated. This issue can be potentially addressed with realistic ocean models. However, the relatively common practice in forced ocean models to relax model sea surface salinity to seasonal climatology to prevent model drift may suppress simulated low-frequency changes of upper ocean salinity.

Our study indicates that having knowledge of the forcing from the Indian and Pacific Oceans are insufficient to understand sea level changes in the southeast Indian Ocean on decadal and perhaps even longer time scales. Reliable estimates of forcing from the Maritime Continent region are indispensible. These include changes in the regional water cycle (river runoff and precipitation), changes in the structure of the ITF, the interaction between the ITF and other elements of the regional circulations such as the Luzon Strait throughflow that regulates the amount of fresh water from the South China Sea into the Makassar Strait [*Gordon et al*., 2012], and the interaction of atmospheric and oceanic features in the Maritime Continent region with climate variability such as El Niño–Southern Oscillation, Pacific Decadal Oscillation, monsoon, and

Indian Ocean Dipole. It is therefore imperative to enhance and sustain the oceanic and atmospheric measurements in the Maritime Continent region, especially the Indonesian Seas. Recent advances in salinity remote sensing such as Aquarius/SAC-D and Soil Moisture and Ocean Salinity satellite missions are expected to benefit related research in the future.

Acknowledgments
William Llovel was supported by University of California at Los Angeles, Joint Institute for Regional Earth System Science and Engineering (JIFRESSE), Los Angeles, CA 90024, USA. We sincerely thank Arnold Gordon for his insight in estimating the advective time scales associated with the ITF based on the pathway of the ITF and related velocity measurements. The altimeter products were produced by Ssalto/*Duacs* and distributed by *AVISO*, with support from *CNES* (http://www.aviso.altimetry.fr/duacs/). The Argo data were collected and made freely available by the International Argo Program and the national programs that contribute to it (http://www.argo.ucsd.edu and http://argo.jcommops.org). The Argo Program is part of the Global Ocean Observing System. NCEP_Reanalysis 2 and GPCP data provided by the NOAA/OAR/ESRL PSD, Boulder, Colorado, USA, from their Web site at http://www.esrl.noaa.gov/psd/. The global ocean evaporation products were provided by the WHOI OAFlux project (http://oaflux.whoi.edu) funded by the NOAA Climate Observations and Monitoring (COM) program. We also thank Paul Durack and an anonymous reviewer for their time and helpful suggestions. The relevant research conducted by Tong Lee was carried out at the Jet Propulsion Laboratory, California Institute of Technology under a contract with the National Aeronautics and Space Administration.

The Editor thanks two anonymous reviewers for their assistance in evaluating this paper.

References

Ablain, M., A. Cazenave, G. Valladeau, and S. Guinehut (2009), A new assessment of the error budget of global mean sea level rate estimated by satellite altimetry over 1993–2008, *Ocean Sci.*, *5*, 193–201, doi:10.5194/os-5-193-2009.

Adler, R. F., et al. (2003), The Version 2 Global Precipitation Climatology Project (GPCP) monthly precipitation analysis (1979-present), *J. Hydrometeorol.*, *4*, 1147–1167.

Argo data management (2011), User's manual, version 2.31. Ar-um-02-01. [Available at www.argodatamgt.org/content/download/9034/61030/file/argo-dm-user-manual-version-2.31.pdf.]

Birol, F., and R. A. Morrow (2003), Separation of quasi-semiannual Rossby waves from the eastern boundary of the Indian Ocean, *J. Mar. Res.*, *61*, 707–723.

Cai, W. J., G. Meyers, and G. Shi (2005), Transmission of ENSO signal to the Indian Ocean, *Geophys. Res. Lett.*, *32*, L05616, doi:10.1029/2004GL021736.

Cazenave, A., and W. Llovel (2010), Contemporary sea level rise, *Annu. Rev. Mar. Sci.*, *2*, 145–173, doi:10.1146/annurev-marine-120308-081105.

Chelton, D. B., and M. G. Schlax (1996), Global observations of oceanic Rossby waves, *Science*, *272*, 234–238, doi:10.1126/science.272.5259.234.

Church, J. A., et al. (2013), Sea level change, in *Climate Change 2013: The Physical Science Basis. Contribution of Working Group I to the Fifth Assessment Report of the Intergovernmental Panel on Climate Change*, edited by T. F. Stocker et al., Cambridge Univ. Press, Cambridge, U. K., and New York, doi:10.1017/CBO9781107415324.026.

Collins, M., et al. (2013), Long-term climate change: Projections, commitments and irreversibility, in *Climate Change 2013: The Physical Science Basis. Contribution of Working Group I to the Fifth Assessment Report of the Intergovernmental Panel on Climate Change*, edited by T. F. Stocker et al., Cambridge Univ. Press, Cambridge, U. K., and New York.

Dee, D. P., et al (2011), The ERA-Interim reanalysis: Configuration and performance of the data assimilation system, *Q. J. R. Meteorol. Soc.*, *137*, 553–597, doi:10.1002/qj.828.

Feng, M., M. J. McPhaden, and T. Lee (2010), Decadal variability of the Pacific subtropical cells and their influence on the southeast Indian Ocean, *Geophys. Res. Lett.*, *37*, L09606, doi:10.1029/2010GL042796.

Gordon, A. L., R. D. Susanto, and K. Vranes (2003), Cool Indonesian throughflow as a consequence of restricted surface layer flow, *Nature*, *425*, 824–828.

Gordon, A. L., J. Sprintall, H. M. van Aken, D. Susanto, S. E. Wijffels, R. Molcard, A. Ffieldf, W. Pranowog, and S. Wirasantosag (2010), The Indonesian throughflow during 2004–2006 as observed by the INSTANT program, *Dyn. Atmos. Oceans*, *50*, 115–128.

Gordon, A. L., B. A. Huber, E. J. Metzger, R. D. Susanto, H. E. Hurlburt, and T. R. Adi (2012), South China Sea throughflow impact on the Indonesian throughflow, *Geophys. Res. Lett.*, *39*, L11602, doi:10.1029/2012GL052021.

Gould, J., et al. (2004), Argo profiling floats bring new era of in situ ocean observations, *Eos Trans. AGU*, *85*(19), 185, doi:10.1029/2004EO190002.

Gregory, J. M., and J. A. Lowe (2000), Predictions of global and regional sea-level rise using AOGCMs with and without flux adjustment, *Geophys. Res. Lett.*, *27*, 3069–3072, doi:10.1029/1999GL011228.

Griffies, S. M., and R. J. Greatbatch (2012), Physical processes that impact the evolution of global mean sea level in ocean climate models, *Ocean Model.*, *51*, 37–72, doi:10.1016/j.ocemod.2012.04.003.

Han, W., et al. (2010), Indian Ocean sea level change in a warming climate, *Nat. Geosci.*, *3*, 118–121, doi:10.1038/ngeo729.

Han, W., J. Vialard, M. J. McPhaden, T. Lee, Y. Masumoto, M. Feng, and W. P. M. de Ruijter (2014), Indian Ocean decadal variability: A review, *Bull. Am. Meteorol. Soc.*, in press.

Kanamitsu, M., W. Ebisuzaki, J. Woollen, S.-K. Yang, J. J. Hnilo, M. Fiorino, and G. L. Potter (2002), NCEP-DOE AMIP-II reanalysis (R-2), *Bull. Am. Meteorol. Soc.*, *83*, 1631–1643.

Kirtman, B., et al. (2013), Near-term climate change: Projections and predictability, in *Climate Change 2013: The Physical Science Basis. Contribution of Working Group I to the Fifth Assessment Report of the Intergovernmental Panel on Climate Change*, edited by T. F. Stocker et al., Cambridge Univ. Press, Cambridge, U. K., and New York.

Koch-Larrouy, A., M. Lengaigne, P. Terray, G. Madec, and S. Masson (2010), Tidal mixing in the Indonesian Seas and its effect on the tropical climate system, *Clim. Dyn.*, *34*(6), 891–904.

Köhl, A. (2014), Detecting processes contributing to interannual halosteric and thermosteric sea level variability, *J. Clim.*, *27*(6), 2417–2426, doi:10.1175/JCLI-D-13-00412.1.

Large, W. G., and S. Pond (1981), Open ocean momentum flux measurements in moderate to strong winds, *J. Phys. Oceanogr.*, *11*, 324–336.

Lee, T. (2004), Decadal weakening of the shallow overturning circulation in the South Indian Ocean, *Geophys. Res. Lett.*, *31*, L18305, doi:10.1029/2004GL020884.

Lee, T., and M. J. McPhaden (2008), Decadal phase change in large-scale sea level and winds in the Indo-Pacific region at the end of the 20th century, *Geophys. Res. Lett.*, *35*, L01605, doi:10.1029/2007GL032419.

Liu, Z. (2012), Dynamics of interdecadal climate variability: A historical perspective, *J. Clim.*, *25*, 1963–1995.

Llovel, W., S. Guinehut, and A. Cazenave (2010), Regional and interannual variability in sea level over 2002–2009 based on satellite altimetry, Argo float data and GRACE ocean mass, *Ocean Dyn.*, *60*, 1193–1204, doi:10.1007/s10236-010-0324-0.

Llovel, W., I. Fukumori, and B. Meyssignac (2013), Depth-dependent temperature change contributions to global mean thermosteric sea level rise from 1960 to 2010, *Global Planet. Change*, *101*, 113–118, doi:10.1016/j.gloplacha.2012.12.011.

Llovel, W., J. K. Willis, F. W. Landerer, and I. Fukumori (2014), Deep-ocean contribution to sea level and energy budget not detectable over the past decade, *Nat. Clim. Change*, *4*(11), 1031–1035, doi:10.1038/nclimate2387.

Lorbacher, K., S. J. Marsland, J. A. Church, S. M. Griffies, and D. Stammer (2012), Rapid barotropic sea level rise from ice sheet melting, *J. Geophys. Res.*, *117*, C06003, doi:10.1029/2011JC007733.

Morrow, R., F. Birol, D. Griffin, and J. Sudre (2004), Divergent pathways of cyclonic and anti-cyclonic ocean eddies, *Geophys. Res. Lett.*, *31*, L24311, doi:10.1029/2004GL020974.

Nicholls, R. J., and A. Cazenave (2010), Sea-level rise and its impacts on coastal zones, *Science*, *328*, 1517.

Nidheesh, A. G., M. Lengaigne, J. Vialard, A. S. Unnikrishnan, and H. Dayan (2013), Decadal and long-term sea level variability in the tropical Indo-Pacific Ocean, *Clim. Dyn.*, *41*, 381–402, doi:10.1007/s00382-012-1463-4.

Qu, T. D., D. Yan, G. Meyers, A. Ishida, and D. Wang (2005), Connecting the tropical Pacific with Indian Ocean through South China Sea, *Geophys. Res. Lett.*, *32*, L24609, doi:10.1029/2005GL024698.

Roemmich, D., and J. Gilson (2009), The 2004-2008 mean and annual cycle of temperature, salinity and steric height in the global ocean from the Argo program, *Prog. Oceanogr.*, *82*, 81–100, doi:10.1016/j.pocean.2009.03.004.

Schwarzkopf, F. U., and C. W. Böning (2011), Contribution of Pacific wind stress to multi-decadal variations in upper ocean heat content and sea level in the tropical south Indian Ocean, *Geophys. Res. Lett.*, *38*, L12602, doi:10.1029/2011GL047651.

Sprintall, J., A. Gordon, A. Koch-Larrouy, T. Lee, J. Potemra, K. Pujiana, and S. Wijffels (2014), The central role of the Indonesian Seas and throughflow in the coupled ocean-climate system, *Nat. Geosci.*, doi:10.1038/ngeo2188.

Stammer, D., A. Cazenave, R. M. Ponte, and M. E. Tamisiea (2013), Causes for contemporary regional sea level changes, *Annu. Rev. Mar. Sci.*, *5*, 21–46, doi:10.1146/annurev-marine-121211-172406.

Tozuka, T., J. Luo, S. Masson, and T. Yamagata (2007), Decadal modulations of the Indian Ocean dipole in the SINTEX-F1 coupled GCM, *J. Clim.*, *20*, 2881–2894.

Trenary, L., and W. Han (2013), Local and remote forcing of decadal sea level and thermocline depth variability in the south Indian Ocean, *J. Geophys. Res. Oceans*, *118*, 381–398, doi:10.1029/2012JC008317.

Wijffels, S., and G. Meyers (2004), An intersection of oceanic waveguides: Variability in the Indonesian throughflow region, *J. Phys. Oceanogr.*, *34*, 1232–1253.

Willis, J. K., D. P. Chambers, and R. S. Nerem (2008), Assessing the globally averaged sea level budget on seasonal to interannual timescales, *J. Geophys. Res.*, *113*, C06015, doi:10.1029/2007JC004517.

Wunsch, C., R. M. Ponte, and P. Heimbach (2007), Decadal trends in sea level patterns: 1993–2004, *J. Clim.*, *20*(24), 5889–5911, doi:10.1175/2007JCLI1840.1.

Yu, L., X. Jin, and R. A. Weller (2008), Multidecade global flux datasets from the objectively analyzed air-sea fluxes (OAFlux) project: Latent and sensible heat fluxes, ocean evaporation, and related surface meteorological variables, Woods Hole Oceanographic Institution, *OAFlux Project Tech. Rep. OA-2008-01,* 64 pp., Woods Hole, Mass.